J Appl Electrochem (2014) 44:1075–1080
DOI 10.1007/s10800-014-0724-9

EDITORIAL

Hydrothermal synthesized micro/nano-sized pyrite used as cathode material to improve the electrochemical performance of thermal battery

Zhaotang Yang · Xiaojiang Liu · Xiuli Feng · Yixiu Cui · Xiaowei Yang

Received: 21 April 2014 / Accepted: 28 July 2014 / Published online: 19 August 2014

Abstract In this paper, single-phase pyrite with different particle sizes is prepared by hydrothermal method with the reactants of Na_2S, S, and $FeSO_4$. Compared with natural pyrite powder, synthesized pyrite nanocubes with small particle sizes and fine distribution have lower resistance, higher specific capacity and power density during the discharging process. The enlarging contacting surface area of pyrite with electrolytes will reduce the concentration polarization caused by the discharging current and improve the utilization efficiency of the pyrite materials. When pulse currents are loaded, compared with natural pyrite single-cell thermal battery, synthetic ones have smaller voltage drops and higher power density during the pulse discharging process. Influences of particle sizes on the thermal stability of the pyrite powders have also been investigated.

Keywords Pyrite nanocubes · Hydrothermal method · Thermal batteries

1 Introduction

Thermal battery is a kind of primary battery working at 450–550 °C with molten salts as electrolytes, which has high power density and reliability. It is widely applied in military weapons [1] as activating power source. Due to low cost, fine compatibility with molten electrolytes and stable discharging stages [2], pyrite made from minerals is the main cathode material for thermal battery. However, the particle sizes of natural pyrite are large and the size distribution is wide (100 nm–100 μm). There are also some impurities mixing with the final products which will affect the discharging performance of the FeS_2/LiSi thermal batteries. Several alternative synthetic methods [3–6] have been investigated in the preparation of pyrite that applied in the thermal batteries. The results show that reducing pyrite particle size will enhance the discharging capacity and power density of the thermal battery, as the larger surface area of synthetic pyrite contacting with electrolytes could effectively reduce the internal resistance of the thermal battery.

Hydrothermal method is an efficient way to prepare uniform inorganic nanoparticles, which provides high temperature and pressure reacting conditions. Thus it can significantly increase the chemical reaction rates [7]. X.F.Qian [8, 9] et al. had prepared nanostructured pyrite with fine distribution via solvothermal process using ethylenediamine as solvent. W.R [10, 11] et al. had prepared FeS_2 with the reactants of $FeSO_4$, S, and $Na_2S_2O_3$ via hydrothermal method, but there are some marcasite (polymorph of pyrite) forming with pyrite at the same time, which will influence the thermal stability of the thermal battery. Recently, Gujie Qian [12] et al. had demonstrated the synthesis of single-phase pyrite via hydrothermal method. However, it is difficult to achieve pyrite from the Fe_3O_4 precursors. We had reported the synthesis of single-phase pyrite via hydrothermal method with the reactants of Na_2S, S, and $FeSO_4$ in the former presentation [13], which avoids the using of organic solvent and Fe_3O_4 precursors. In this paper, by the adjustments of pH, reaction time t, reaction temperatures T, and so on, pyrite with different particle sizes has been successfully synthesized via hydrothermal method. The prepared single-phase pyrite with small particles and fine distribution could reduce the

Z. Yang · X. Liu (✉) · X. Feng · Y. Cui · X. Yang
Institute of Electronic Engineering, China Academy of Engineering Physics, Mianyang 621900, Sichuan, China
e-mail: yztresearch@163.com

impedances and improve the discharging power density of the cathode of the single cells.

2 Experimental

All chemical reagents were of analytical grade and used without further purification. In a typical reaction, 0.02 mol $FeSO_4$ $7H_2O$ and 0.02 mol $Na_2S{\cdot}9H_2O$ were dissolved into 40 ml deionized water. Then 0.02 mol $Na_2S{\cdot}9H_2O$ and 0.02 mol S were dissolved into 30 ml deionized water and heated to 100 °C until no residual sulfur existing [14]. Finally, the solutions prepared above were added into a Teflon liner autoclave of 100 ml capacity and the autoclave was kept at 95–200 °C for 3–24 h at pH 9. The pH of the solution was adjusted by NaOH (1.5 mol L^{-1}) and H_2SO_4 (1.5 mol L^{-1}) solutions. After cooling to room temperature naturally, the solids were washed several times with dilute sulphuric acid and distilled water to remove the residual FeS, then the solid products were added into Na_2S boiling solution to remove the sulfur. After washing the products several times with distilled water and ethanol in turn, the products were dried in vacuum for 3 h at 100 °C.

The powder X-ray diffraction (XRD) patterns were recorded on a Japan Rigaku Damaxg A X-ray diffractometer with Cu Ka radiation ($u = 1.54178$ A). Scanning electron microscope (SEM) images were taken with JSM-6490 and TM-1000 scanning electron microscope. The thermal stability of the hydrothermally synthesized pyrite was investigated by the NETZSCH STA 449C thermogravimetry–differential scanning calorimetry (TG–DSC). The TG–DSC measurement was carried out under the pure Ar atmosphere with heating rate = 10 °C min^{-1}, the sample weight is about 10 mg.

The single-cell thermal battery (FeS_2/LiSi) consists of cathode (0.2 g FeS_2), eutectic salt electrolytes (0.2 g LiCl–KCl) and anode (0.1 g LiSi). Since the synthetic pyrite could not form pellet directly by cold press, MgO was added to improve the cathode viscidity. The cathode materials consist of 50 % FeS_2, 35 % eutectic salt mixture (LiCl–KCl), and 15 % MgO. The electrolytes were a mixture of 70 % eutectic salt mixture (LiCl–KCl) and 30 % MgO. Here MgO is used to retard the melted electrolyte from following out of the cells. The anode was Li–Si alloys and they were commercially available. 4 MPa static pressure was used to press natural cathode to pellets. Since the loosing synthetic pyrite is difficult to compress, 6 MPa was applied to keep synthetic cathode pellets having the same thickness as natural cathode pellets. The materials of electrolyte and anode were spreaded layer by layer, graphite papers were used at bottom of the cell to collect the current. The diameter of the thermal battery is 17 mm.

The KENWOOD DDS60-6 and Agilent 6060B DC electronic load have been employed to provide the constant current. Agilent 34,401 A has been used to monitor potential variations between the anode and cathode of cells during the discharging process. The discharge experiments were carried out under 500 °C. Three experiments were taken at each current density to ensure the reliability of the discharging data of the single-cell thermal battery.

3 Results

3.1 Synthesis of pyrite with different particle sizes

Figure 1 shows the SEM images of single-phase pyrite with different particle sizes. At the condition of pH 10, $T = 120$ °C, $t = 12$ h, the particle size of the prepared pyrite is about 80 nm. Figure 1a shows that the pyrite particles having flake-like morphology. At the condition of pH 10, $T = 160$ °C, $t = 24$ h, pyrite particles with cubic morphology were prepared and the particle size was about 250 nm (Fig. 1b). At the condition of pH 9, $T = 160$ °C, $t = 24$ h, pyrite particle with cubic morphology was prepared and the particle size was about 700 nm (Fig. 1d). From Fig. 1a–c it can be seen that the synthetic pyrite particles are well distributed and the agglomeration [15] of the pyrite particles are not serious. Figure 1d shows the image of natural pyrite. Compared with pyrite prepared via hydrothermal method, the natural pyrite has larger particle sizes, and the distribution of the particle size is wide (100 nm–100 μm, according to the laser particle size analysis). Furthermore, the morphologies of the particles are irregular. The laser particle size investigation shows that the average diameter of the particles is about 27 μm (Fig. 1e). Compared with natural pyrite, synthetic pyrite has larger specific surface area, which may improve the contacting surface with electrolytes and has a better electrochemical performance when discharging at large current density.

Figure 2a–c show the XRD patterns of synthetic iron disulfide with different particle sizes, the peaks of all the synthetic samples can be indexed to a pure-phase pyrite (JCPDS No. 42–1340). Figure 2d shows that the iron disulfide bought from commercial company is cubic-phase pyrite.

3.2 Discharge experiments

To evaluate the electrochemical performance of synthetic pyrite, the single-cell thermal batteries consisting of synthesized pyrite and natural pyrite discharged at different current densities.

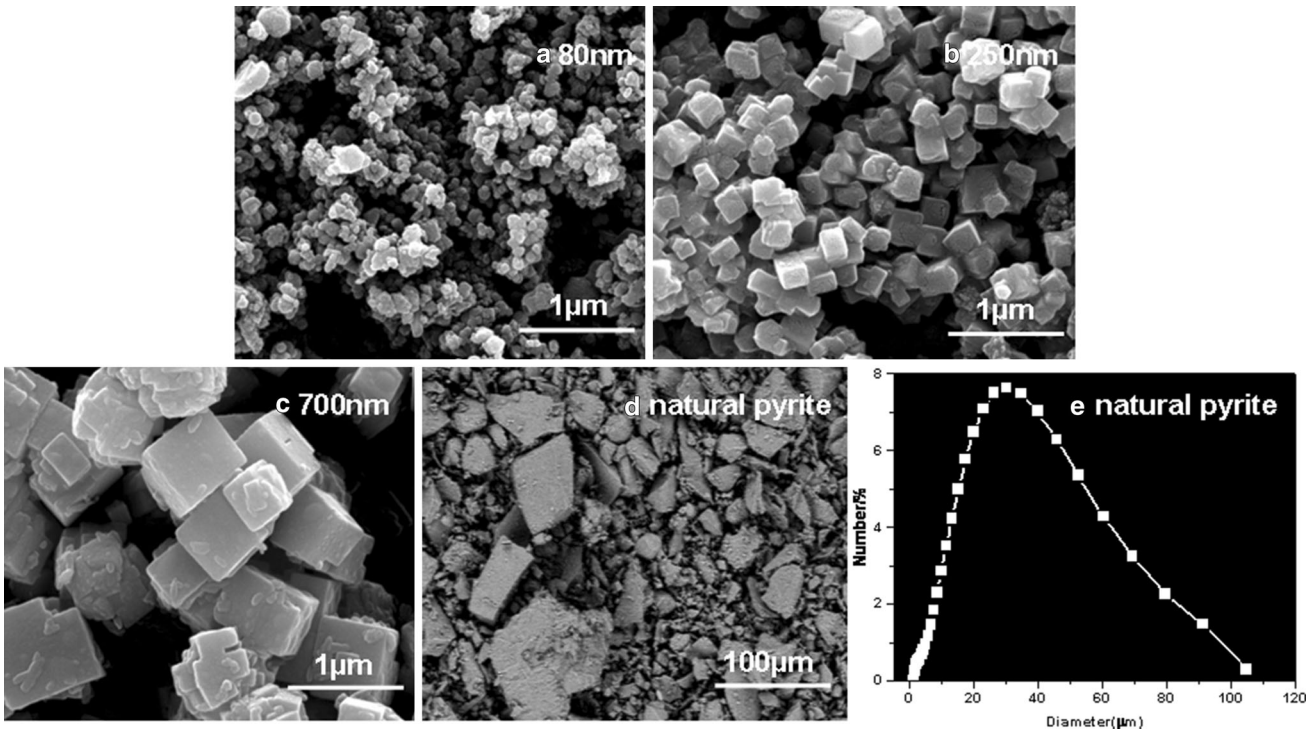

Fig. 1 SEM images of pyrite with different sizes **a** 80 nm; **b** 250 nm; **c** 700 nm; **d** natural pyrite; **e** laser particle size analysis of natural pyrite

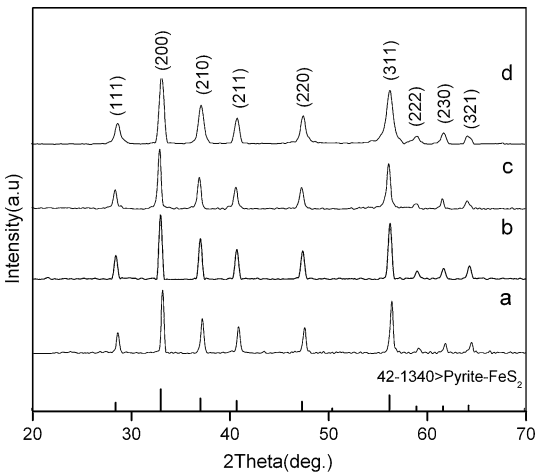

Fig. 2 XRD patterns of the iron disulfide: *a* 80 nm; *b* 250 nm *c* 700 nm; *d* natural pyrite

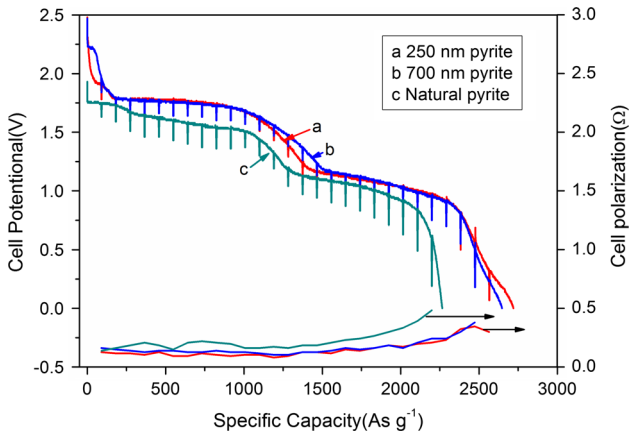

Fig. 3 Polarization of the single-cell thermal batteries with synthetic and natural pyrite. Current density: 0.5 A cm^{-2}; pulse current density: 1 A cm^{-2}

3.2.1 Polarization of the thermal cells

In order to evaluate the polarization of the single-cell thermal batteries, 1 A cm^{-2} pulse current density was applied to the battery test each 10 s while the battery discharging at 0.5 A cm^{-2} constant current density (Fig. 3). For the synthetic pyrite, when the specific capacity of the thermal battery is smaller than 1,200 As g^{-1}, the resistance of the thermal battery is stable for both natural and synthetic pyrite. After 1,200 As g^{-1}, the resistance of the thermal battery increases gradually as the electrical resistivity of the discharging products increasing at the same time [2]. The polarization curves reveal that the resistance of the thermal battery made of the synthetic pyrite is smaller than that of the natural counterpart. The single-cell thermal battery of 250-nm pyrite has smaller resistance than that of 700-nm pyrite single-cell thermal battery as the particle sizes decrease. The pyrite with small particle sizes own lager contacting surface area with molten electrolytes,

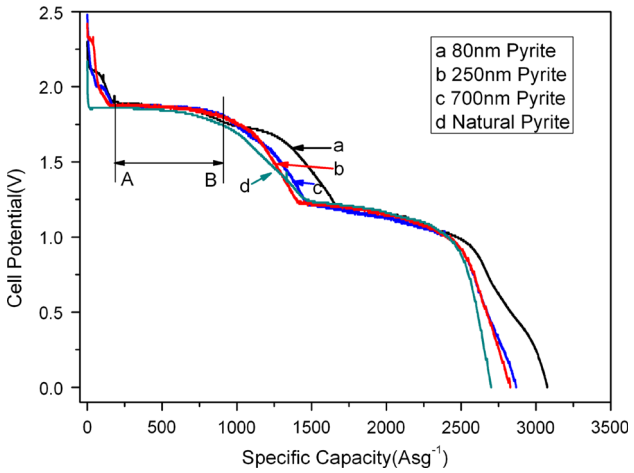

Fig. 4 Discharge curves of natural and synthetic pyrite with different particle sizes under 500 °C at 0.2 A cm^{-2}

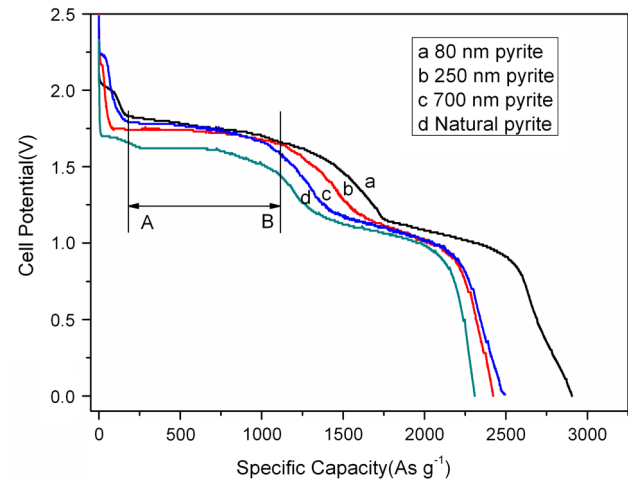

Fig. 5 Discharge curves of natural and synthetic pyrite under 500 °C at 0.5 A cm^{-2}

then the current of the unite area will reduce at the same discharging current, which will reduce the concentration polarization between the pyrite particles and electrolytes interface. As a result, the polarization of the thermal battery will reduce, and the voltage of the battery will be improved.

3.2.2 *Constant current discharging*

The discharging curves of natural and hydrothermally synthesized pyrite samples are shown in Figs. 4 and 5. The discharging constant current density was 0.2 and 0.5 A cm^{-2}.

A voltage spike was formed in the early discharge stages for both natural and synthetic pyrite, which was described in J.P.Pemsler's article [4]. The FeS_2 thermal batteries usually pick up the first discharging stage as the working

Table 1 The average voltage improvements of synthetic pyrite comparing with natural pyrite thermal batteries between AB region under 0.2 and 0.5 A cm^{-2}

	ΔU (mV/0.2 A cm^{-2})	ΔU (mV/0.5 A cm^{-2})
80 nm	30	175
250 nm	22	131
700 nm	19	144
Natural pyrite	/	/

stages, so in the following discussion we focus on the electrochemical performance of the first discharging stage. Table 1 lists the average voltage improvements of the synthetic pyrite thermal batteries comparing with the natural pyrite thermal battery between AB region at 0.2 A cm^{-2} (as shown in Fig. 4) and 0.5 A cm^{-2} (as shown in Fig. 5). Taking 80-nm pyrite as an example, the ΔU at 0.2 A cm^{-2} is 30 mV, as the discharging current density increased to 0.5 A cm^{-2}, the ΔU becomes larger at same time, which is 175 mV. The 80-nm pyrite has larger contacting surface area with electrolytes than natural pyrite, which will reduce the concentration polarization between the electrolytes and the pyrite interfaces. This is in accordance with the polarization changes showed in Fig. 3. As the discharging current increases, the polarization caused by the limited natural pyrite surface area contacting with the electrolytes become more obvious, as a result, the ΔU increases with increasing discharging current, 30 mV at 0.2 A cm^{-2} and 175 mV at 0.5 A cm^{-2}. In addition, at 0.2 and 0.5 A cm^{-2} discharging current density, the ΔU shows increasing trend with the decreasing pyrite particle sizes. Table 2 lists the discharging specific capacity and power density of the thermal batteries at 0.5 A cm^{-2}. I_s is the improvement of the discharging specific capacity of the synthetic pyrite than that of the natural one, and I_p is the improvement of the discharging power density of the synthetic pyrite than that of the natural one. Taking 80-nm thermal battery as an example, the discharging specific capacity and power density are 1,462 As g^{-1} and 0.71 Wh g^{-1}, which increase 40 and 47 %, respectively, comparing with the natural samples. From Table 2, we can see that when the particle sizes

Table 2 Specific capacity and power density of the thermal batteries at 1.5 V voltage cutoff

	Specific capacity (As g^{-1})	Power density (Wh g^{-1})	I_s (%)	I_s (%)
80 nm	1,462	0.71	40	47
250 nm	1,289	0.62	23	28
700 nm	1,200	0.59	15	23
Natural pyrite	1,044	0.48	/	/

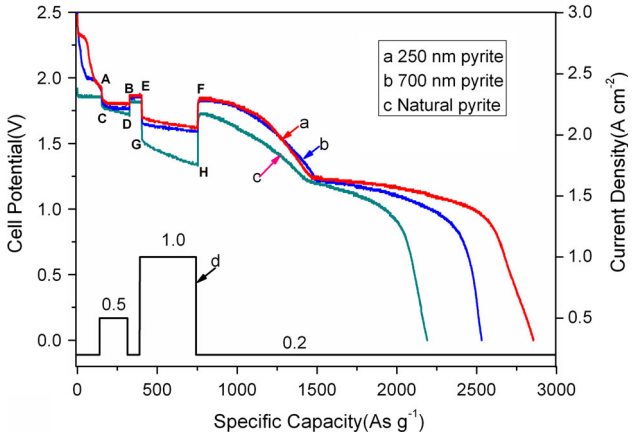

Fig. 6 Polarization of thermal cells with synthetic and natural pyrite. Current density: 0.5 A cm^{-2}; pulse current density: 1 A cm^{-2}. *a* 250-nm pyrite; *b* 700-nm pyrite; *c* natural pyrite; *d* discharging current curves of thermal cells

decreasing, the specific capacity of the thermal batteries increases gradually. As the particle sizes decrease, the specific surface area of the pyrite materials increases, the amount of the pyrite materials taking part in the electrochemical reactions will increase, as a result, the specific capacity of the pyrite material increases. Synthetic pyrite owns bigger specific surface area than that of natural pyrite due to its smaller particle size, which leads to larger contacting surface area with electrolyte. As discussed above, improving the contacting surface area between the pyrite and the electrolyte is helpful in reducing the polarization of the thermal battery, which results in the improvement of the discharging voltages. This improvement is more obvious when the single-cell thermal battery discharging under large current density. As displayed in Fig. 5, the discharging voltage plateaus of synthetic pyrite are higher and more stable than that of the natural one.

3.2.3 Pulse current discharging

As discussed above, synthetic pyrite nanocubes with fine distribution show excellent electrochemical performance when discharging at large current density. In this part, the single-cell thermal battery discharging at 0.2 A cm^{-2} constant current density, 0.5 and 1 A cm^{-2} pulse current density were loaded to evaluate the discharging performance of the thermal batteries under large current density condition (Fig. 6). Figure 6 shows the discharging curve of the single-cell thermal battery. U_{ij} was calculated by the following equation, Table 3 lists the U_{ij} of the different pyrite thermal batteries. $U_{ij} = U_{i-}U_{j.}$ *i* is A, E in Fig. 6. *j* is D, H in Fig. 6. U_{AD} is the total voltage drop when 0.5 A cm^{-2} pulse current was loaded. U_{EH} is the total voltage drop when 1 A cm^{-2} pulse current was loaded.

Table 3 The total voltage drop when pulse current is loaded

	U_{AD}	U_{EH}
250-nm pyrite	0.11	0.24
650-nm pyrite	0.13	0.26
Natural pyrite	0.14	0.48

At 0.5 A cm^{-2} pulse current density, the voltage drops of synthetic pyrite and natural pyrite are similar, and U_{AF} increases with increasing pyrite particle sizes. As the pulse current density increases to 1 A cm^{-2}, the gap of the voltage drop (U_{CH}) between the synthetic pyrite and the natural pyrite becomes larger, and the U_{CH} voltage drop of the natural pyrite is 1.8 times larger than that of the 650-nm synthetic pyrite. Figure 3 shows that between 150 and 300 As g^{-1}, the polarization of the natural thermal battery and synthetic one are familiar, which lead the closed voltage drops at 0.5 A cm^{-2} pulse current density. When 1 A cm^{-2} pulse current density was loaded, the polarization of the natural pyrite battery is larger than that of the synthetic pyrite battery between 400 and 750 As g^{-1} (Fig. 3), so the voltage drops are larger than those of the synthetic pyrite thermal batteries. Synthetic pyrite with small particle sizes and fine distribution can reduce the polarization of the thermal batteries while discharging at large current density. The synthesized pyrite battery has higher power density than the natural one. At 1.5 V voltage cutoff, the discharging specific capacity of natural pyrite is 1,177 As g^{-1}; the discharging specific capacity of 250-nm pyrite is 1,307 As g^{-1}, and the discharging specific capacity of 700-nm pyrite is 1,312 As g^{-1}, which shows that synthetic pyrite has larger discharging specific capacity than the natural one. After the large pulse current discharging, the natural pyrite single-cell thermal battery discharging voltage is low and not stable. On the contrary, the synthetic pyrite single-cell thermal battery shows much longer discharging time and higher discharging voltage.

3.3 Thermal stability of the pyrite materials

TG–DSC (Fig. 7) analysis was used to investigate the thermal stability of synthetic and natural pyrite. As shown in Fig. 7, 80-nm pyrite starts to decompose at 200 °C, and significant decomposition takes place at 614 °C; 700-nm pyrite starts to decompose at 509 °C, and significant decomposition takes place at 623 °C; natural pyrite starts to decompose at 506 °C, and significant decomposition takes place at 627 °C. The TG results indicated that the starting decomposition temperature of the pyrite material decreases as the particle size reduces, this may be caused by the increasing specific area of the pyrite which have influence on the decomposition process of the pyrite material. Nano pyrite with large surface area will increase

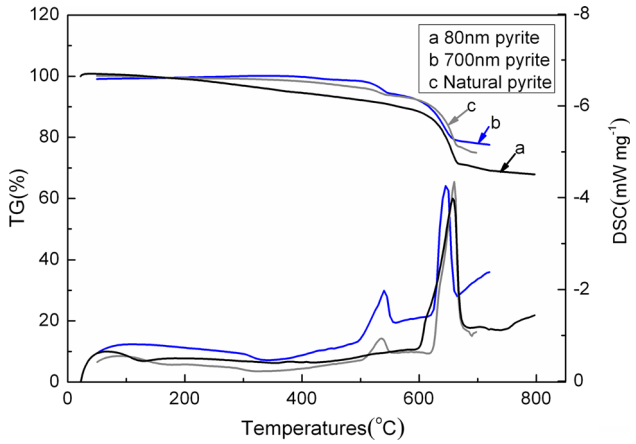

Fig. 7 TG–DSC curves of natural and synthetic pyrite with pure Ar atmosphere

the reactivity of the materials, then the material can reach the decomposition S_n species [2] partial pressure at a lower temperature, which leads to a lower decomposition temperature of the pyrite materials.

4 Conclusions

Single-phase pyrite has been synthesized via the reactants of Na_2S, S, and $FeSO_4$. With the adjustments of pH, reacting time, and temperatures, 80-nm flake-like pyrite particles, 250- and 700-nm pyrite particles with cubic morphology have been successfully prepared. The discharging experiments show that the single-cell thermal batteries consisting of the synthetic pyrite with fine distribution had lower polarization than that of the natural sample. When discharging at large current density, the synthetic pyrite has higher discharging voltage and larger specific capacity than that of the natural pyrite-based single-cell thermal battery; at the discharging condition of 0.5 A cm^{-2} constant current density, 1.5 V voltage cutoff, the specific capacity and power density of the 80-nm pyrite are 1,462 As g^{-1} and 0.71 Wh g^{-1}, which are 1.40 and 1.47 times of natural pyrite-based single-cell thermal batteries. The pulse current discharging experiments show that the 250- and 700-nm pyrite could reduce the total voltage drop and enhance the discharging voltage during the discharging process. The small voltage drop and the high discharging voltage is beneficial to improve the reliability and designability of the thermal battery. The TG–DSC analysis reveals that the pyrite decomposition temperature shows decreasing trend as the particle sizes decreasing. The 250- and 700-nm pyrite show great potential for the application of high power density and long life thermal batteries technology.

Acknowledgments This project was financially supported by the Pre-Research Foundation of China Academy of Engineering Physics under Contract No. 426030405.

References

1. Guidotti RA, Masset PJ (2006) J Power Sources 161:1443–1449
2. Masset PJ, Guidotti RA (2008) J Power Sources 177:595–609
3. Guidotti RA, Reinhardt FW, Dai J (2006) J Power Sources 160:1456–1464
4. Pemsler JP, Lam RKF, Litchfield JK (1990) J Electrochem Soc 137:1–7
5. Ming A (2003) J Power Sources 115:360–366
6. Guidotti RA, Reinhardt FW (2002) Material Research Society Symposium. Proceedings 730
7. Byrappa K, Adschiri T (2007) Prog Cryst Growth Ch 53:117–166
8. Qian XF, Zhang XM, Wang C (1999) Mater Sci Eng B 64:170–173
9. Qian XF, Xie Y, Qian YT (2001) Mater Lett 48:109–111
10. Wu R, Zheng YF, Zhang XG (2004) J Cryst Growth 266:523–527
11. Duan H, Zheng YF, Dong YZ (2004) Mater Res Bull 39:1861–1868
12. Qian GJ, Brugger J, Skinner WM (2010) Geochim Cosmochim Acta 74:5610–5630
13. Yang ZT, Liu XJ, Liu JS et al (2013) Key Eng Mater 562–565:136
14. Yao FY (1998) Inorganic chemical series. Science Press, Beijing
15. Butler A, Rickard D (2000) Geochim Cosmochim Acta l64:2665–2672